The UV and visible spectra of chlorine peroxide : constraining the atmospheric photolysis rate

Young, I. A. K.; Jones, R. L.; Pope, Francis

DOI:
10.1002/2013GL058626

Document Version
Publisher final version (usually the publisher pdf)

Citation for published version (Harvard):
Young, IAK, Jones, RL & Pope, FD 2014, 'The UV and visible spectra of chlorine peroxide : constraining the atmospheric photolysis rate' Geophysical Research Letters, vol 41, no. 5, pp. 1781–1788., 10.1002/2013GL058626

AGU PUBLICATIONS

Geophysical Research Letters

RESEARCH LETTER
10.1002/2013GL058626

Key Points:
- Powerful new laboratory technique for resolving weak and overlapping spectra
- First measurement of the combined UV and visible spectra of ClOOCl
- Determination of the ClOOCl photolysis rate

Supporting Information:
- Readme
- Table S1
- Text S1
- Figure S1
- Figure S2
- Figure S3

Correspondence to:
F. D. Pope,
f.pope@bham.ac.uk

Citation:
Young, I. A. K., R. L. Jones, and F. D. Pope (2014), The UV and visible spectra of chlorine peroxide: Constraining the atmospheric photolysis rate, *Geophys. Res. Lett.*, *41*, doi:10.1002/2013GL058626.

Received 7 NOV 2013
Accepted 26 JAN 2014
Accepted article online 29 JAN 2014

The UV and visible spectra of chlorine peroxide: Constraining the atmospheric photolysis rate

I. A. K. Young[1], R. L. Jones[1], and F. D. Pope[2]

[1]Centre for Atmospheric Science, Department of Chemistry, University of Cambridge, Cambridge, UK, [2]School of Geography, Earth and Environmental Sciences, University of Birmingham, Edgbaston, UK

Abstract The photolysis of chlorine peroxide (ClOOCl) is a key chemical step in the depletion of polar stratospheric ozone. As such, precise measurements of the absorption cross sections for ClOOCl are required. In this paper we provide two critical pieces of laboratory data with which to constrain the rate of ozone depletion. First, we provide an optically pure ClOOCl spectrum in the photolytically important UV wavelength region (200–350 nm). Second, we provide the first ever measurement of the ClOOCl spectrum in the visible region (509–536 nm) conclusively demonstrating the photolysis of ClOOCl to be negligible in this spectral region. The visible measurement is important because it can be used to anchor other previously recorded UV spectra and hence reduce the uncertainty in the ClOOCl photolysis rate. The calculated photolysis rate from this study indicates that the current models of stratospheric ozone depletion are correct.

1. Introduction

1.1. Chlorine Peroxide and Ozone Depletion

The springtime destruction of polar ozone (O_3) was first observed by *Farman et al*. [1985], and this destruction continues to the present day [*World Meteorological Organization* (*WMO*), 2011]. The link between ozone depletion and the presence of halogen, and in particular chlorine, containing gases in the stratosphere was quickly elucidated after the *Farman et al*. publication and ultimately led to the phasing out of the chlorine-containing chlorofluorocarbon gases through the 1989 Montreal Protocol and subsequent treaties [*WMO*, 2011].

The photolysis of the ClOOCl molecule is the rate-limiting step in the formation of the chlorine oxide species (ClOx = ClO + Cl), which are responsible for the majority of the ozone depletion in the stratospheric polar springtime [*Solomon*, 1999; *von Hobe et al*., 2013]. During winter months, the stratosphere is dark and cold thereby allowing ClOOCl to form as a reservoir species of the more reactive ClOx which catalytically destroy O_3 [*Molina and Molina*, 1987]. The return of light in spring to the polar regions initiates the destruction of the photolabile ClOOCl thereby regenerating ClOx. The key reactions in the generation and loss of ClOOCl are shown below in reactions (R1–R3).

$$\mathrm{ClO} + \mathrm{ClO} + M \leftrightarrows \mathrm{ClOOCl} + M \quad \text{R1, R-1 (at low temperature RHS is favored.)}$$

$$\mathrm{ClOOCl} + \mathrm{hv} \rightarrow \mathrm{ClOO} + \mathrm{Cl} \quad \text{R2 (slow)}$$

$$\mathrm{ClOO} + M \rightarrow \mathrm{Cl} + \mathrm{O_2} + M \quad \text{R3 (rapid)}$$

The photolysis rate of ClOOCl (J_{ClOOCl}) is calculated by equation (E1), where σ_{ClOOCl} is the absorption cross section, ϕ_{ClOOCl} is the photolysis quantum yield, F is the actinic flux, and λ is the wavelength. The quantum yield [*Huang et al*., 2011; *Moore et al*., 1999; *Plenge et al*., 2004] has been sufficiently investigated through previous laboratory measurements as stated in *Sander et al*. [2011]. The actinic fluxes can be modeled, both spatially and temporally, to a high accuracy (e.g., MYSTIC) [*Mayer*, 2009].

$$J_{\mathrm{ClOOCl}} = \int \sigma_{\mathrm{ClOOCl}}(\lambda)\phi_{\mathrm{ClOOCl}}(\lambda)F(\lambda)d\lambda \quad \text{(E1)}$$

1.2. Previous Spectral Determinations of ClOOCl

There have been numerous measurements of the ClOOCl absorption cross section, and these are shown in Figures S1 and S2 of the supporting information [*Bloss et al*., 2001; *Burkholder et al*., 1990; *Chen et al*., 2009; *Cox and Hayman*, 1988; *DeMore and Tschuikow-Roux*, 1990; *Huder and DeMore*, 1995; *Jin et al*., 2010; *Lien et al*., 2009; *Papanastasiou et al*., 2009; *Pope et al*., 2007; *von Hobe et al*., 2009; *Wilmouth et al*., 2009]. Large

discrepancies still exist between the different laboratory determinations of the absorption cross sections of ClOOCl in the long-wavelength tail region. In particular, the study of *Pope et al*. [2007] was controversial because of its very low proposed values [*Pope et al*., 2007], which if correct, would indicate that the photolysis of ClOOCl was too slow to explain the generation of ClOx required to generate the observed polar ozone depletions [*Schiermeier*, 2007; *von Hobe*, 2007]. The *Pope et al*. study highlighted the lack of scientific consensus on the ClOOCl absorption cross section and renewed interest in the laboratory measurement of ClOOCl. Subsequently, six new studies measured the UV absorption cross sections using a variety of advanced techniques [*Chen et al*., 2009; *Jin et al*., 2010; *Lien et al*., 2009; *Papanastasiou et al*., 2009; *von Hobe et al*., 2009; *Wilmouth et al*., 2009]. However, within these studies, there are still significant differences between measurements at wavelengths longer than 300 nm (see Figure S2 of the supporting information). Currently, the Jet Propulsion Laboratory (JPL) kinetics evaluation [*Sander et al*., 2011] recommends the ClOOCl spectrum reported by *Papanastasiou et al*. [2009], recorded in the wavelength range 200–420 nm. At longer wavelengths, a log linear extrapolation of the *Papanastasiou et al*. data is recommended [*Sander et al*., 2011]. The *Papanastasiou et al*. study used diode array spectroscopy and isosbestic points to remove the contribution of the Cl_2 absorbance from the spectrum of the Cl_2/ClOOCl gas mixture [*Papanastasiou et al*., 2009].

One of the greatest difficulties in measuring the ClOOCl spectrum is generating pure ClOOCl within the laboratory. The synthetic routes employed involve precursors (e.g., Cl_2, O_3, and Cl_2O) and generate coproducts (e.g., OClO and Cl_2O_3) which are also absorbed in the UV/visible region (see Figure S3 of the supporting information). Distillation has been utilized as an effective method for removing most of the impurities [*Pope et al*., 2007]. However, Cl_2 is stubbornly resistant to complete removal because the vapor pressure is similar to ClOOCl. Furthermore, the Cl_2 spectrum is smooth, broad, and similar to ClOOCl, making it problematic to unambiguously subtract from the ClOOCl spectrum. Several studies have employed indirect measures of the absorption cross section, which remove the importance of spectral impurities [*Chen et al*., 2009; *Jin et al*., 2010; *Lien et al*., 2009; *Wilmouth et al*., 2009]. Unfortunately, these studies rely on powerful lasers which can only be utilized at discrete wavelengths, and thus, the complete ClOOCl spectrum cannot be elucidated.

Prior to this study, the longest wavelength measurement of ClOOCl was 420 nm [*Papanastasiou et al*., 2009]. Theoretical calculations suggest that there is a possibility of additional electronic transitions occurring in the long-wavelength tail of the spectrum [*Peterson and Francisco*, 2004; *Stanton and Bartlett*, 1993]. Absorptions of low magnitude at long wavelengths could be significant because of the greater actinic flux in the visible region of the spectrum compared to the UV region. The recent stratospheric aircraft campaign carried out in the RECONCILE project [*von Hobe et al*., 2013] indirectly indicated that the long-wavelength tail of the ClOOCl spectrum should be photolytically negligible at wavelengths longer than 420 nm [*Suminska-Ebersoldt et al*., 2012].

2. Materials and Methods

2.1. Experimental Strategy

This study utilizes a twin-channel spectrometer [*Young et al*., 2011] to make absorption measurements of ClOOCl and Cl_2 mixtures in both the UV (200–350 nm) and visible (509–536 nm) spectral regions. The UV channel utilizes conventional single-pass spectroscopy, and the visible channel exploits the highly sensitive Cavity-Enhanced Absorption Spectroscopy (CEAS) technique [*Engeln et al*., 1998; *Langridge et al*., 2008; *O'Keefe*, 1998] to measure the much weaker spectrum of Cl_2 in the visible part of the spectrum.

The experimental strategy was to generate mixtures of ClOOCl and Cl_2 using the methodology of *Pope et al*. [2007], then optimize the ClOOCl:Cl_2 ratio through distillation and temperature-dependent desorption of the mixture from a cold trap. The highly structured and well-characterized visible Cl_2 spectrum [*Maric et al*., 1993; *Young et al*., 2011] allows for the unambiguous measurement of the temporally evolving Cl_2 concentration.

Once the concentration of Cl_2 is known, the absorption due to Cl_2 in both spectral regions can be calculated, through knowledge of the UV and visible absorption cross sections, and subtracted from the composite ClOOCl/Cl_2 spectra resulting in pure ClOOCl spectra. The UV reference spectrum is taken from 2011 JPL kinetics evaluation [*Sander et al*., 2011], and the visible spectrum is taken from the study of *Young et al*. [2011]. This study did not measure the absolute concentration of ClOOCl within the absorption cell. The peak UV absorption, measured at 244 nm, is scaled to the corresponding peak absorption cross section recommended

by the 2010 JPL kinetics evaluation [*Sander et al*., 2011], which is based on the study of *Papanastasiou et al*. [2009]. Hence, the measurements reported herein are subject to the stated ±35% uncertainty of the JPL recommendation.

2.2. Experiment

The dual-beam spectrometer apparatus has been described in detail before [*Young et al*., 2011], and only a brief description is given here. The apparatus is composed of three distinct sequential sections: a photolysis cell in which ClOOCl is generated, a cold temperature trap in which to purify ClOOCl, and an absorption cell in which to measure ClOOCl and the optical impurities. All three components are temperature controlled. Throughout all stages of the experiment, the total flow through the photolysis cell, trap, and absorption cell was maintained at ~2 L/min and was controlled by mass flow controllers (MKS). A schematic diagram of the dual-beam spectrometer can be found in the study of *Young et al*. [2011].

Within the photolysis cell, ClOOCl is generated via the photolysis of Cl_2 in the presence of O_3. The reaction mechanism is shown in reactions (R4–R6), where *M* is any third body collision partner. The resulting mixture is composed of the following optically absorbing gases: ClOOCl, Cl_2, O_3, and trace amounts of OClO and Cl_2O_3. Higher oxides may also be present but were not spectroscopically identified.

$$Cl_2 + h\nu(UV) \rightarrow 2Cl \quad \text{(R4)}$$

$$Cl + O_3 \rightarrow ClO + O_2 \quad \text{(R5)}$$

$$ClO + ClO + M \rightarrow ClOOCl + M \quad \text{(R6)}$$

The cold trap was constructed from quartz, and its initial trapping temperature was set at ~150 K. This allowed for the capture of ClOOCl, Cl_2, and higher ClOx species while allowing O_3, which possesses a higher vapor pressure, to escape. Correspondingly, there was no spectroscopic evidence of codeposition of O_3 within the trap. Once sufficient ClOOCl has been collected, the trap is warmed to release the trapped gas into the absorption cell. The trap is slowly warmed, with a typical ramp rate of ~1 K min^{-1}, to an upper trap temperature which led to the release of ClOOCl and Cl_2 but no other spectral impurities. The OClO and Cl_2O_3 species leave the trap at higher temperatures and thus were not observed under the experimental conditions.

The vapor pressure of Cl_2 is greater than ClOOCl, and therefore, Cl_2 leaves the cold trap at lower temperatures than ClOOCl. This physical difference between Cl_2 and ClOOCl was exploited to increase the concentration ratio of the desorbed ClOOCl:Cl_2 entering the absorption cell which is kept at a constant temperature of 197 K. Conditions were optimized to produce a desorption period which contained high ClOOCl concentrations (up to ~4×10^{12} cm^{-3}) combined with low Cl_2 concentrations. Complete separation of the ClOOCl and Cl_2 is not achieved, and hence, all raw spectra contain some influence from the Cl_2 contaminant.

Both spectroscopic channels operate simultaneously and sample the same gas mixture. The combination of the visible and UV channels allows for the subtraction of the Cl_2 absorbance from both channels. In the UV channel, both Cl_2 and ClOOCl have similar shaped broad structureless spectra in the wavelength range ~300–360 nm (see Figure S3 of the supporting information) making it impossible to subtract the Cl_2 signal unambiguously without further information. This extra information is acquired from the visible spectrum, where the clear structure of Cl_2 (see Figure 1) allows for the determination of the Cl_2 concentration. The values of the absorption cross sections of the visible Cl_2 spectrum are temperature dependent; therefore, a pure reference spectrum is required and is provided by *Young et al*. [2011]. Knowledge of the Cl_2 concentration allows for the subtraction of the Cl_2 absorbance within both the visible and UV spectra resulting in the pure ClOOCl spectra.

Within the absorption cell, the UV absorbance (A_{UV}) of the gas mixture is measured using single-pass spectroscopy and follows the Beer-Lambert relationship (for *i* different absorbers) given in equation (E2), where *I* and I_0 are the intensities of light transmitted through the cell with and without the absorbers present, respectively. The *l* is the path length, $\sigma(\lambda)$ is the wavelength-dependent absorption cross section, and *c* is the concentration of absorber.

$$A_{UV} = \ln\frac{I_0}{I} = \Sigma_i \sigma_i \; l \; c_i \quad \text{(E2)}$$

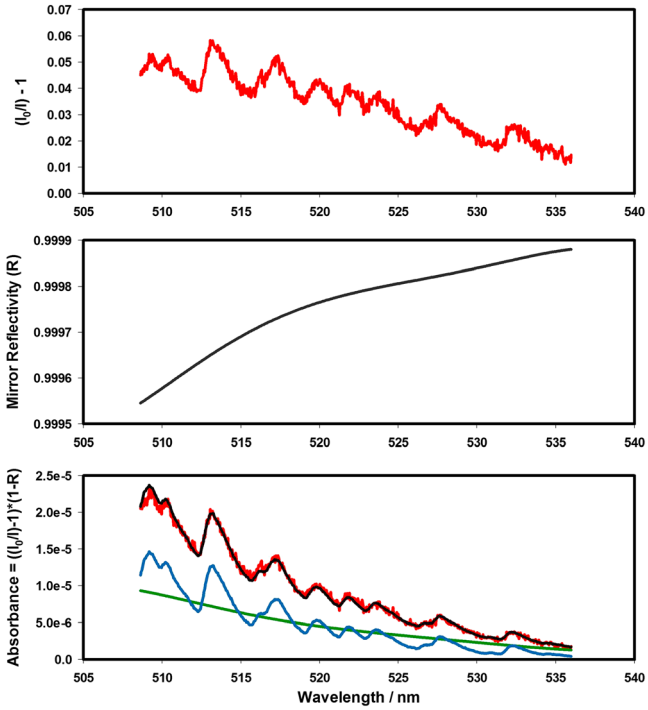

Figure 1. Cavity-enhanced absorption spectra of ClOOCl and Cl_2. (top) The laboratory-measured spectrum of a ClOOCl + Cl_2 mixture of path integral concentrations of ClOOCl and $Cl_2 = 4.1 \times 10^{16}$ cm^{-2} and 1.6×10^{17} cm^{-2}, respectively. For a given wavelength: (I_0/I)-1 $= \sum_i \sigma_i l c_i/(1\text{-}R)$. (middle) The BBCEAS mirror reflectivity obtained from a spectrum of pure Cl_2 of known concentration. (bottom) The absorbance spectra of the ClOOCl + Cl_2 mixture and individual ClOOCl and Cl_2 components: red line: laboratory-measured spectrum of ClOOCl + Cl_2 mixture, black line: fitted spectrum of ClOOCl + Cl_2 mixture, blue line: fitted Cl_2 spectrum, and green line: fitted ClOOCl spectrum.

The absorbance of the gas mixture in the visible channel has a much lower absorbance and hence is measured with the ultra sensitive BroadBand Cavity-Enhanced Absorption Spectroscopy (BBCEAS) technique. Figure 1 illustrates how the absorbance, due only to ClOOCl, is obtained from the visible spectrum. The wavelength-dependent absorbance of the ClOOCl and Cl_2 mixture can be calculated from the intensity of light transmitted through the BBCEAS channel with (I) and without (I_0) the absorbers present and the mirror reflectivity (R) via equation (E3) which is valid under conditions of low absorbance [*Fiedler et al.*, 2003]. The BBCEAS mirror reflectivity, and hence the effective path length for each experiment, was determined by recording a spectrum of pure Cl_2 of known concentration. We previously measured the temperature-dependent high-resolution absorption cross sections of Cl_2, as documented by *Young et al.* [2011], and these values are used to determine the effective mirror reflectivity for these experiments. The path integral concentration of Cl_2 (Cl_2 concentration multiplied by path length) is obtained from the UV measurement of Cl_2.

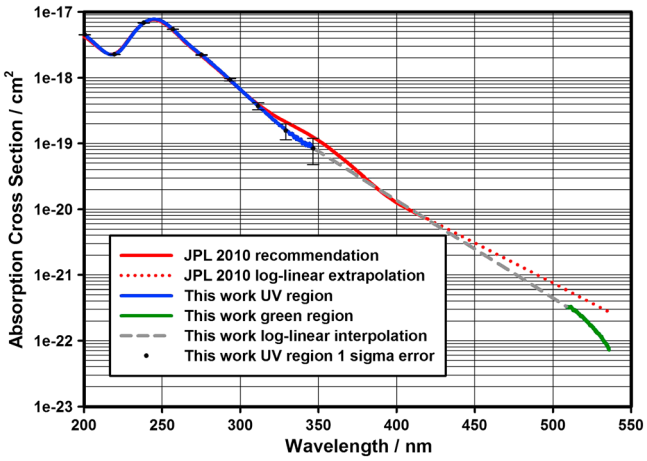

Figure 2. Visible and UV absorption cross sections of ClOOCl. The interpolation between the UV and green measurements from this study is log linear with boundary conditions provided by the longest wavelength UV measurement and shortest wavelength green measurement.

$$A_{vis} = \left(\frac{I_0}{I} - 1\right)(1 - R) \quad \text{(E3)}$$

Once the absorbance spectrum of the Cl_2 and ClOOCl mixture is known, the relative contribution from Cl_2 can be

Table 1. UV and Visible Absorption Cross Sections of ClOOCl at 197 K[a]

Wavelength (nm)	Absorption Cross Section (cm^2)	1σ Standard Deviation (cm^2)
200	4.47E–18	2.39E–20
205	3.54E–18	2.08E–20
210	2.76E–18	1.86E–20
215	2.26E–18	1.66E–20
220	2.22E–18	1.46E–20
225	2.81E–18	1.30E–20
230	4.08E–18	1.43E–20
235	5.71E–18	1.96E–20
240	7.08E–18	2.58E–20
245	7.58E–18	2.97E–20
250	7.02E–18	3.00E–20
255	5.79E–18	2.86E–20
260	4.48E–18	2.79E–20
265	3.43E–18	2.88E–20
270	2.70E–18	3.10E–20
275	2.17E–18	3.39E–20
280	1.75E–18	3.69E–20
285	1.38E–18	3.96E–20
290	1.09E–18	4.08E–20
295	8.37E–19	4.22E–20
300	6.50E–19	4.32E–20
305	5.06E–19	4.42E–20
310	3.92E–19	4.49E–20
315	3.05E–19	4.51E–20
320	2.38E–19	4.44E–20
325	1.84E–19	4.34E–20
330	1.48E–19	4.22E–20
335	1.25E–19	4.06E–20
340	9.98E–20	3.85E–20
345	9.12E–20	3.65E–20
510	3.21E–22	1.80E–23
515	2.77E–22	1.64E–23
520	2.12E–22	1.50E–23
525	1.61E–22	1.35E–23
530	1.19E–22	1.17E–23
535	8.20E–23	9.15E–24

[a]High-resolution data interpolated onto a 5 nm grid using air wavelengths. The standard deviation does not take into account the uncertainty on the normalized peak cross section.

easily subtracted because of its highly structured spectrum in the wavelength region 509–535 nm. At longer wavelengths, the amount of structure diminishes; hence, the retrieval error increases, and as such, we only report the spectrum for the highly structured region. This retrieval of the Cl_2 absorbance provides the Cl_2 concentration, since the absorption cross sections and path length are known, which can then be used to subtract the correct amount of Cl_2 from the visible spectrum. The residual spectrum, that is left once the Cl_2 contribution has been subtracted from the composite (ClOOCl + Cl_2) spectrum, consistently possesses the same shape that is well fitted to a polynomial of order 4. The chronology of the appearance and the changing magnitude of the residual spectrum are synchronous with the UV spectrum of ClOOCl. Therefore, we confidently attribute the residual spectrum to be the visible absorbance spectrum of ClOOCl. The absolute absorption cross sections are obtained by normalizing the absorbance spectrum with the same factor used for the UV spectrum. This approach is valid because the same gas is being sampled in both the UV and visible channels.

The gases used in this study were used without further purification: 5% Cl_2/N_2 (BOC), O_2 (BOC), and N_2 (BOC). The O_3 was generated from the photolysis of synthetic air using a mercury lamp (Penray lamp).

3. Results and Discussion

The UV and visible absorption cross sections of pure ClOOCl are shown in Figure 2 and are compared to the most recent 2010 JPL recommendation [*Sander et al.*, 2011]. Table 1 provides the averages and the 1σ

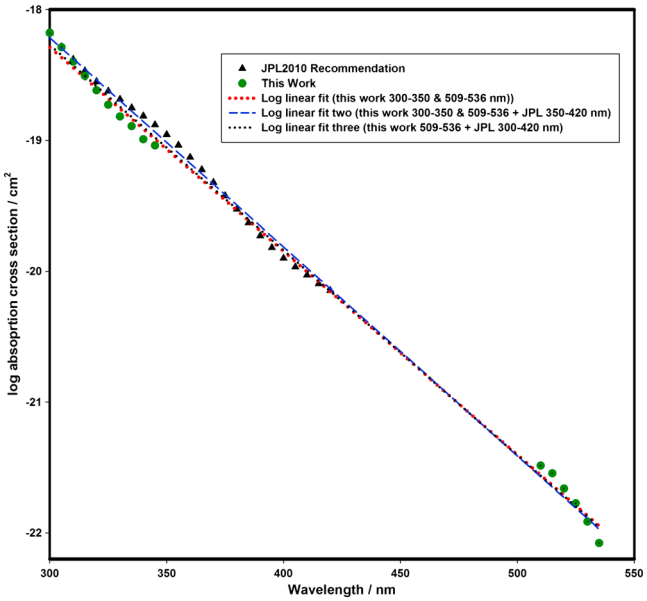

Figure 3. ClOOCl absorption cross sections in the photolytically important wavelength region ($\lambda > 300$ nm). The JPL recommendation is based upon the work of *Papanastasiou et al*. [2009]. Three different interpolations are used to fill the data gap between the laboratory measurements: interpolation 1 (red dotted line) uses only the UV and visible data from this study leaving a data gap between 350 and 509 nm. Interpolation 2 uses the UV and visible data from this study in addition to the *Papanastasiou et al*. data in the range 350–420 nm leaving a data gap between 420 and 509 nm. Interpolation 3 uses the UV data of *Papanastasiou et al*. and the visible data from this study leaving a data gap between 420 and 509 nm.

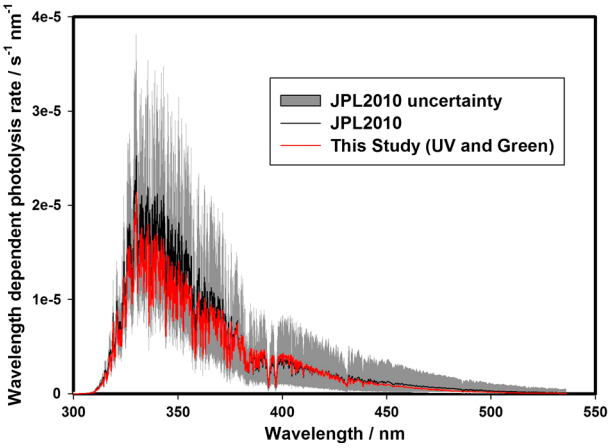

Figure 4. Wavelength-dependent ClOOCl photolysis rates in the polar stratosphere. The photolysis rates are calculated using equation (E1). The quantum yield (Φ) for reaction (R2) is set equal to 0.8 as recommended by the JPL kinetics evaluation [*Sander et al*., 2011]. High-resolution actinic flux (F) data are obtained from the output of the MYSTIC model used with the following model parameters: altitude = 20 km, no aerosol or clouds, ozone concentration = 350 Dobson unit, surface albedo = 0.3, and solar zenith angle = 85°[*Mayer*, 2009]. MYSTIC is operated as one of several solvers of the libRadtran radiative transfer package [*Mayer and Kylling*, 2005]. The spectra were calculated in a fully spherical geometry [*Emde and Mayer*, 2007] using the absorption line importance sampling method [*Emde et al*., 2011]. The JPL 2010 recommendation [*Sander et al*., 2011] for the absorption cross sections is based upon the laboratory work of *Papanastasiou et al*. [2009] and uses a log linear extrapolation at wavelengths longer than 420 nm. The uncertainty on the JPL recommendation represents the consensus of the panel members on JPL kinetics evaluation committee [*Sander et al*., 2011]. The absorption cross sections from this work are the interpolated data from the combined UV and green data sets (blue, pink, and green lines in Figure 2).

standard deviations for both the UV and visible ClOOCl absorption cross sections interpolated to a resolution of 5 nm. Higher-resolution (0.5 nm) spectral data are provided in the supporting information.

The measured UV ClOOCl spectrum is slightly weaker, at wavelengths long of 300 nm, than the JPL-recommended *Papanastasiou et al.* [2009] data but falls within its stated uncertainty. This study provides the first measurement of the visible ClOOCl spectrum. The spectrum is found to be broad and unstructured; it rapidly reduces in intensity with increasing wavelength. A log linear interpolation between the UV and visible data sets is shown in Figure 2. This combination of the UV and visible data suggests that the absorption cross section of ClOOCl follows an approximately log linear relationship with wavelength at wavelengths longer than 300 nm. This result is consistent with the absence of additional nonnegligible electronic transitions occurring at wavelengths longer than 300 nm. However, it should be noted that this study cannot rule out additional absorption features appearing in the ~159 nm data gap between 350 and 509 nm.

The good agreement, within errors, between this study and the study of *Papanastasiou et al.* [2009], which extends the long UV measurement to 420 nm, allows for the combination of data sets to reduce the laboratory data gap to 89 nm (420–509 nm), which further constrains the ClOOCl photolysis rate. Figure 3 highlights the measured and interpolated absorption spectra of ClOOCl in the photolytically important wavelength region. It can be seen that the visible measurement, provided by this study, effectively anchors the data and removes much of the uncertainty within the long-wavelength tail of ClOOCl assuming a log linear relationship holds over the whole wavelength range. This is consistent with the RECONCILE field measurements which suggested that it is unlikely that any photolytically significant absorption will exist at wavelengths longer than 420 nm [*Suminska-Ebersoldt et al.*, 2012]. However, even a small additional peak ($>1\times10^{-20}$ cm^2) in the unmeasured 420–509 nm region could significantly increase the photolysis rate due to the high actinic flux present at these wavelengths.

Figure 4 compares the wavelength-dependent photolysis rates, relevant for the polar arctic stratospheric spring, derived from the interpolated absorption cross section data measured in this study and the recommended JPL evaluation values including the recommended extrapolation at wavelengths longer than 420 nm. The calculated photolysis rate for ClOOCl integrated over all relevant UV and visible wavelengths detailed in Figure 3 is found to be 7.3×10^{-4} s^{-1}, approximately 22% lower than the current JPL recommendation, but it is well within the stated uncertainty of the JPL recommendation [*Sander et al.*, 2011]. The absorption cross sections measured in the green region of the spectrum are found to be too small to be photolytically important. However, as previously stated, their major value is to anchor the UV data measurements and hence provide a powerful constraint upon the overall photolysis rate of ClOOCl.

4. Conclusions

The photolysis of chlorine peroxide (ClOOCl) is a key chemical step in the depletion of polar stratospheric ozone. This study provides an optically pure ClOOCl spectrum in the photolytically important UV wavelength region (200–350 nm) that is in good agreement with other recently published spectra. Second, the study provides the first ever measurement of the ClOOCl spectrum in the visible region (509–536 nm) conclusively demonstrating the photolysis of ClOOCl to be negligible in this spectral region. The visible measurement can be used to anchor other previously recorded UV spectra and hence reduce the uncertainty in ClOOCl photolysis rate calculations. The calculated photolysis rate from this study indicates that current models of stratospheric ozone depletion are correct. Furthermore, the new visible spectrum measurement greatly improves the confidence in this result.

Acknowledgments
This work was funded through the EU FP7 RECONCILE project (grant: RECONCILE-226365-FP7-ENV-2008-1). Exploratory funding for this project was provided through the FP6 SCOUT-O3 project. We thank Marc von Hobe and Fred Stroh for their hospitality and many stimulating discussions. Tony Cox is thanked for his useful advice and interest in this project. MYSTIC radiative transfer calculations were kindly provided by Claudia Emde.

The Editor thanks two anonymous reviewers for their assistance in evaluating this paper.

References

Bloss, W. J., S. L. Nickolaisen, R. J. Salawitch, R. R. Friedl, and S. P. Sander (2001), Kinetics of the ClO self-reaction and 210 nm absorption cross section of the ClO dimer, *J. Phys. Chem. A*, *105*(50), 11,226–11,239.

Burkholder, J. B., J. J. Orlando, and C. J. Howard (1990), Ultraviolet-absorption cross-sections of Cl_2O_2 between 210 and 410 nm, *J. Phys. Chem.-Us*, *94*(2), 687–695.

Chen, H. Y., C. Y. Lien, W. Y. Lin, Y. T. Lee, and J. J. Lin (2009), UV absorption cross sections of ClOOCl are consistent with ozone degradation models, *Science*, *324*(5928), 781–784.

Cox, R. A., and G. D. Hayman (1988), The stability and photochemistry of dimers of the ClO radical and implications for Antarctic ozone depletion, *Nature*, *332*(6167), 796–800.

DeMore, W. B., and E. Tschuikow-Roux (1990), Ultraviolet-spectrum and chemical-reactivity of the ClO dimer, *J. Phys. Chem.-Us*, *94*(15), 5856–5860.

Emde, C., and B. Mayer (2007), Simulation of solar radiation during a total eclipse: a challenge for radiative transfer, *Atmos. Chem. Phys.*, *7*(9), 2259–2270.
Emde, C., R. Buras, and B. Mayer (2011), ALIS: An efficient method to compute high spectral resolution polarized solar radiances using the Monte Carlo approach, *J. Quant. Spectros. Radiat. Transfer*, *112*(10), 1622–1631.
Engeln, R., G. Berden, R. Peeters, and G. Meijer (1998), Cavity enhanced absorption and cavity enhanced magnetic rotation spectroscopy, *Rev. Sci. Instrum.*, *69*(11), 3763–3769.
Farman, J. C., B. G. Gardiner, and J. D. Shanklin (1985), Large losses of total ozone in Antarctica reveal seasonal ClOx/NOx interaction, *Nature*, *315*(6016), 207–210.
Fiedler, S. E., A. Hese, and A. A. Ruth (2003), Incoherent broad-band cavity-enhanced absorption spectroscopy, *Chem. Phys. Lett.*, *371*(3–4), 284–294.
Huang, W.-T., A. F. Chen, I. C. Chen, C.-H. Tsai, and J. J.-M. Lin (2011), Photodissociation dynamics of ClOOCl at 248.4 and 308.4 nm, *Phys. Chem. Chem. Phys.*, *13*(18), 8195–8203.
Huder, K. J., and W. B. DeMore (1995), Absorption cross-sections of the ClO dimer, *J. Phys. Chem.-Us*, *99*(12), 3905–3908.
Jin, B., I. C. Chen, W. T. Huang, C. Y. Lien, N. Guchhait, and J. J. Lin (2010), Photodissociation cross section of ClOOCl at 330 nm, *J. Phys. Chem. A*, *114*(14), 4791–4797.
Langridge, J. M., S. M. Ball, A. J. L. Shillings, and R. L. Jones (2008), A broadband absorption spectrometer using light emitting diodes for ultrasensitive, in situ trace gas detection, *Rev. Sci. Instrum.*, *79*(12), 123110.
Lien, C. Y., W. Y. Lin, H. Y. Chen, W. T. Huang, B. Jin, I. C. Chen, and J. J. Lin (2009), Photodissociation cross sections of ClOOCl at 248.4 and 266 nm, *J. Chem. Phys.*, *131*(17), 174301.
Maric, D., J. P. Burrows, R. Meller, and G. K. Moortgat (1993), A study of the UV-visible absorption-spectrum of molecular chlorine, *J. Photochem. Photobiol., A*, *70*(3), 205–214.
Mayer, B. (2009), Radiative transfer in the cloudy atmosphere, *EPJ Web Conf.*, *1*, 75–99.
Mayer, B., and A. Kylling (2005), Technical note: The libRadtran software package for radiative transfer calculations - description and examples of use, *Atmos. Chem. Phys.*, *5*(7), 1855–1877.
Molina, L. T., and M. J. Molina (1987), Production of Cl_2O_2 from the self-reaction of the ClO radical, *J. Phys. Chem.-Us*, *91*(2), 433–436.
Moore, T. A., M. Okumura, J. W. Seale, and T. K. Minton (1999), UV photolysis of ClOOCl, *J. Phys. Chem. A*, *103*(12), 1691–1695.
O'Keefe, A. (1998), Integrated cavity output analysis of ultra-weak absorption, *Chem. Phys. Lett.*, *293*(5-6), 331–336.
Papanastasiou, D. K., V. C. Papadimitriou, D. W. Fahey, and J. B. Burkholder (2009), UV absorption spectrum of the ClO dimer (Cl2O2) between 200 and 420 nm, *J. Phys. Chem. A*, *113*(49), 13,711–13,726.
Peterson, K. A., and J. S. Francisco (2004), Does chlorine peroxide absorb below 250 nm?, *J. Chem. Phys.*, *121*(6), 2611–2616.
Plenge, J., R. Flesch, S. Kühl, B. Vogel, R. Müller, F. Stroh, and E. Rühl (2004), Ultraviolet photolysis of the ClO dimer, *J. Phys. Chem. A*, *108*(22), 4859–4863.
Pope, F. D., J. C. Hansen, K. D. Bayes, R. R. Friedl, and S. P. Sander (2007), Ultraviolet absorption spectrum of chlorine peroxide, ClOOCl, *J. Phys. Chem. A*, *111*(20), 4322–4332.
Sander, S. P., et al. (2011), Chemical kinetics and photochemical data for use in atmospheric studies, Evaluation No. 17*Rep.*, Jet Propulsion Laboratory, Pasadena, Calif.
Schiermeier, Q. (2007), Chemists poke holes in ozone theory, *Nature*, *449*(7161), 382–383.
Solomon, S. (1999), Stratospheric ozone depletion: A review of concepts and history, *Rev. Geophys.*, *37*(3), 275–316.
Stanton, J. F., and R. J. Bartlett (1993), Does chlorine peroxide exhibit a strong ultraviolet-absorption near 250 nm, *J. Chem. Phys.*, *98*(12), 9335–9339.
Suminska-Ebersoldt, O., et al. (2012), ClOOCl photolysis at high solar zenith angles: Analysis of the RECONCILE self-match flight, *Atmos. Chem. Phys.*, *12*(3), 1353–1365.
von Hobe, M. (2007), Atmospheric science - Revisiting ozone depletion, *Science*, *318*(5858), 1878–1879.
von Hobe, M., F. Stroh, H. Beckers, T. Benter, and H. Willner (2009), The UV/Vis absorption spectrum of matrix-isolated dichlorine peroxide, ClOOCl, *Phys. Chem. Chem. Phys.*, *11*(10), 1571–1580.
von Hobe, M., et al. (2013), Reconciliation of essential process parameters for an enhanced predictability of Arctic stratospheric ozone loss and its climate interactions (RECONCILE): Activities and results, *Atmos. Chem. Phys.*, *13*(18), 9233–9268.
Wilmouth, D. M., T. F. Hanisco, R. M. Stimpfle, and J. G. Anderson (2009), Chlorine-catalyzed ozone destruction: Cl atom production from ClOOCl photolysis, *J. Phys. Chem. A*, *113*(51), 14,099–14,108.
WMO (2011), Scientific assessment of ozone depletion: 2010, Global Ozone Research and Monitoring Project-Report No. 52, 516 pp., Geneva, Switzerland.
Young, I. A. K., C. Murray, C. M. Blaum, R. A. Cox, R. L. Jones, and F. D. Pope (2011), Temperature dependent structured absorption spectra of molecular chlorine, *Phys. Chem. Chem. Phys.*, *13*(33), 15,318–15,325.